

Supporting Information for “Explainable Fragment-based Molecular Property Attribution”

Lingxiang Jia¹, Zunlei Feng¹, Haotian Zhang¹, Jie Song¹, Zipeng Zhong¹, Shaolun Yao¹,
and Mingli Song¹

¹Zhejiang University

May 16, 2022



figures/si-activation/si-activation-eps-converted-to.pdf

Figure 1: **Figure S1. The distribution of attribution activations for the 12 tasks on Tox21 dataset.** The blue points denote positive sample activations, and the red ones denote negative.

figures/si-fragment-1/si-fragment-1-eps-converted-to.pdf

Figure 2: **Figure S2. Attribution results of fragment-based method for ‘Hepatobiliary disorders’ task (1/4).** The red highlight displays the crucial fragments or atoms for certain molecule. The three columns (from left to right) respectively denote the ‘Ground Truth’ fragment from the literature, the atom-based attribution result, and the fragment-based attribution result. References [1([Smith et al., 2003](#)), 2([Usui et al., 2009](#))] give the related literature. The top-10 attribution atoms is shown for ‘Atom-based’ method, and ‘Top-k’ denotes that the fragment ranks the k-th highest in the overall results for the molecule.

figures/si-fragment-2/si-fragment-2-eps-converted-to.pdf

Figure 3: **Figure S3. Attribution results of fragment-based method for ‘Hepatobiliary disorders’ task (2/4).** The red highlight displays the crucial fragments or atoms for certain molecule. The three columns (from left to right) respectively denote the ‘Ground Truth’ fragment from the literature, the atom-based attribution result, and the fragment-based attribution result. References [2(Usui et al., 2009), 3(Remmel et al., 2007), 4(Kassahun et al., 2001)] give the related literature. The top-10 attribution atoms is shown for ‘Atom-based’ method, and ‘Top- k’ denotes that the fragment ranks the k-th highest in the overall results for the molecule.

figures/si-fragment-3/si-fragment-3-eps-converted-to.pdf

Figure 4: **Figure S4. Attribution results of fragment-based method for ‘Hepatobiliary disorders’ task (3/4).** The red highlight displays the crucial fragments or atoms for certain molecule. The three columns (from left to right) respectively denote the ‘Ground Truth’ fragment from the literature, the atom-based attribution result, and the fragment-based attribution result. References [5(Uetrecht et al., 1995), 6(Geneve et al., 1987), 7(Wong et al., 2000)] give the related literature. The top-10 attribution atoms is shown for ‘Atom-based’ method, and ‘Top- k’ denotes that the fragment ranks the k-th highest in the overall results for the molecule.

figures/si-fragment-4/si-fragment-4-eps-converted-to.pdf

Figure 5: **Figure S5. Attribution results of fragment-based method for ‘Hepatobiliary disorders’ task (4/4).** The red highlight displays the crucial fragments or atoms for certain molecule. The three columns (from left to right) respectively denote the ‘Ground Truth’ fragment from the literature, the atom-based attribution result, and the fragment-based attribution result. References [1([Smith et al., 2003](#)), 5([Utrecht et al., 1995](#)), 6([Geneve et al., 1987](#)), 7([Wong et al., 2000](#)), 8([Nelson et al., 1976](#))] give the related literature. The top-10 attribution atoms is shown for ‘Atom-based’ method, and ‘Top-k’ denotes that the fragment ranks the k-th highest in the overall results for the molecule.



figures/si-fragment-5/si-fragment-5-eps-converted-to.pdf

Figure 6: **Figure S6. Attribution results of fragment-based method for ‘Congenital, familial and genetic disorders’ task (1/4).** The red highlight displays the crucial fragments or atoms for certain molecule. The three columns (from left to right) respectively denote the ‘Ground Truth’ fragment from the literature, the atom-based attribution result, and the fragment-based attribution result. References [9(Kazius et al., 2005), 10(Bailey et al., 2005)] give the related literature. The top-10 attribution atoms is shown for ‘Atom-based’ method, and ‘Top-k’ denotes that the fragment ranks the k-th highest in the overall results for the molecule.

figures/si-fragment-6/si-fragment-6-eps-converted-to.pdf

Figure 7: **Figure S7. Attribution results of fragment-based method for ‘Congenital, familial and genetic disorders’ task (2/4).** The red highlight displays the crucial fragments or atoms for certain molecule. The three columns (from left to right) respectively denote the ‘Ground Truth’ fragment from the literature, the atom-based attribution result, and the fragment-based attribution result. References [9(Kazius et al., 2005), 11(Benigni & Bossa, 2008), 12(Corvaro et al., 2020)] give the related literature. The top-10 attribution atoms is shown for ‘Atom- based’ method, and ‘Top-k’ denotes that the fragment ranks the k-th highest in the overall results for the molecule.

figures/si-fragment-7/si-fragment-7-eps-converted-to.pdf

Figure 8: **Figure S8. Attribution results of fragment-based method for ‘Congenital, familial and genetic disorders’ task (3/4).** The red highlight displays the crucial fragments or atoms for certain molecule. The three columns (from left to right) respectively denote the ‘Ground Truth’ fragment from the literature, the atom-based attribution result, and the fragment-based attribution result. References [10(Bailey et al., 2005), 11(Benigni & Bossa, 2008), 13(Mariotti et al., 2013)] give the related literature. The top-10 attribution atoms is shown for ‘Atom- based’ method, and ‘Top-k’ denotes that the fragment ranks the k-th highest in the overall results for the molecule.

figures/si-fragment-8/si-fragment-8-eps-converted-to.pdf

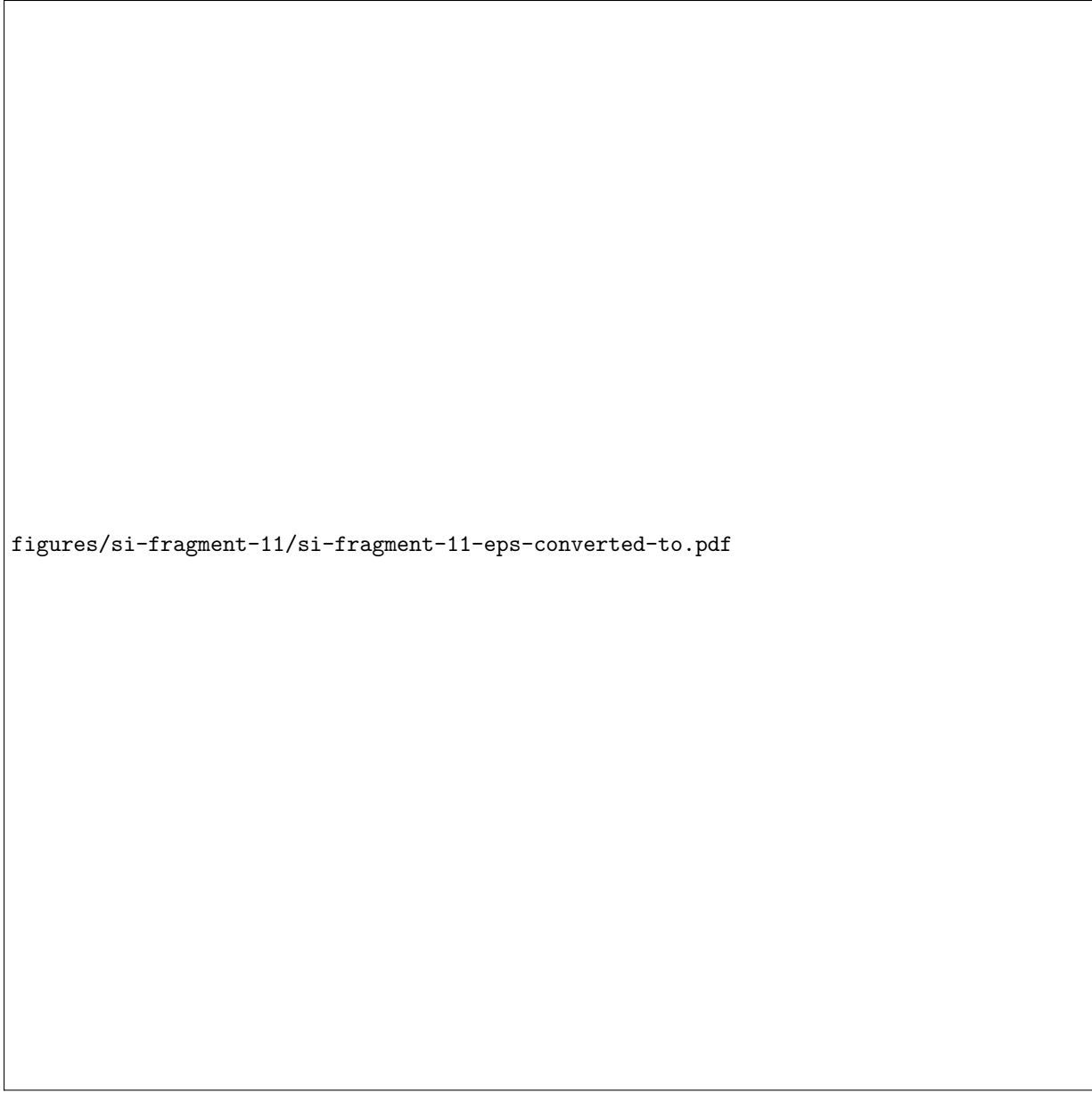
Figure 9: **Figure S9. Attribution results of fragment-based method for ‘Congenital, familial and genetic disorders’ task (4/4).** The red highlight displays the crucial fragments or atoms for certain molecule. The three columns (from left to right) respectively denote the ‘Ground Truth’ fragment from the literature, the atom-based attribution result, and the fragment-based attribution result. References [9(Kazius et al., 2005), 13(Mariotti et al., 2013)] give the related literature. The top-10 attribution atoms is shown for ‘Atom-based’ method, and ‘Top-k’ denotes that the fragment ranks the k-th highest in the overall results for the molecule.

figures/si-fragment-9/si-fragment-9-eps-converted-to.pdf

Figure 10: **Figure S10. S10. Attribution results of fragment-based method for ‘Skin and subcutaneous tissue disorders’ task (1/3).** The red highlight displays the crucial fragments or atoms for certain molecule. The three columns (from left to right) respectively denote the ‘Ground Truth’ fragment from the literature, the atom-based attribution result, and the fragment-based attribution result. References [14([Enoch et al., 2008](#))] give the related literature. The top-10 attribution atoms is shown for ‘Atom-based’ method, and ‘Top-k’ denotes that the fragment ranks the k-th highest in the overall results for the molecule.

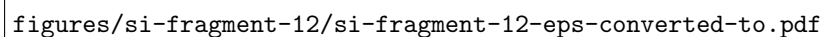
figures/si-fragment-10/si-fragment-10-eps-converted-to.pdf

Figure 11: **Figure S11. Attribution results of fragment-based method for ‘Skin and subcutaneous tissue disorders’ task (2/3).** The red highlight displays the crucial fragments or atoms for certain molecule. The three columns (from left to right) respectively denote the ‘Ground Truth’ fragment from the literature, the atom-based attribution result, and the fragment-based attribution result. References [14([Enoch et al., 2008](#)), 15([Payne & Walsh, 1994](#))] give the related literature. The top-10 attribution atoms is shown for ‘Atom-based’ method, and ‘Top-k’ denotes that the fragment ranks the k-th highest in the overall results for the molecule.



figures/si-fragment-11/si-fragment-11-eps-converted-to.pdf

Figure 12: **Figure S12. Attribution results of fragment-based method for ‘Skin and subcutaneous tissue disorders’ task (3/3).** The red highlight displays the crucial fragments or atoms for certain molecule. The three columns (from left to right) respectively denote the ‘Ground Truth’ fragment from the literature, the atom-based attribution result, and the fragment-based attribution result. References [14(Enoch et al., 2008)] give the related literature. The top-10 attribution atoms is shown for ‘Atom-based’ method, and ‘Top-k’ denotes that the fragment ranks the k-th highest in the overall results for the molecule.



figures/si-fragment-12/si-fragment-12-eps-converted-to.pdf

Figure 13: **Figure S13. Attribution results of fragment-based method for ‘Blood and lymphatic system disorders’ task (1/2).** The red highlight displays the crucial fragments or atoms for certain molecule. The three columns (from left to right) respectively denote the ‘Ground Truth’ fragment from the literature, the atom-based attribution result, and the fragment-based attribution result. References [16(Stepan et al., 2011), 17(van N, 2003)] give the related literature. The top-10 attribution atoms is shown for ‘Atom-based’ method, and ‘Top-k’ denotes that the fragment ranks the k-th highest in the overall results for the molecule.

figures/si-fragment-13/si-fragment-13-eps-converted-to.pdf

Figure 14: **Figure S14. Attribution results of fragment-based method for ‘Blood and lymphatic system disorders’ task (2/2).** The red highlight displays the crucial fragments or atoms for certain molecule. The three columns (from left to right) respectively denote the ‘Ground Truth’ fragment from the literature, the atom-based attribution result, and the fragment-based attribution result. References [16(Stepan et al., 2011), 17(van N, 2003), 18(Notley et al., 2002)] give the related literature. The top-10 attribution atoms is shown for ‘Atom-based’ method, and ‘Top-k’ denotes that the fragment ranks the k-th highest in the overall results for the molecule.

figures/si-fragment-14/si-fragment-14-eps-converted-to.pdf

Figure 15: **Figure S15. Attribution results of fragment-based method for ‘Endocrine disorders’ task (1/3).** The red highlight displays the crucial fragments or atoms for certain molecule. The three columns (from left to right) respectively denote the ‘Ground Truth’ fragment from the literature, the atom-based attribution result, and the fragment-based attribution result. References [19(Nendza et al., 2016)] give the related literature. The top-10 attribution atoms is shown for ‘Atom-based’ method, and ‘Top-k’ denotes that the fragment ranks the k-th highest in the overall results for the molecule.

figures/si-fragment-15/si-fragment-15-eps-converted-to.pdf

Figure 16: **Figure S16. Attribution results of fragment-based method for ‘Endocrine disorders’ task (2/3).** The red highlight displays the crucial fragments or atoms for certain molecule. The three columns (from left to right) respectively denote the ‘Ground Truth’ fragment from the literature, the atom-based attribution result, and the fragment-based attribution result. References [19(Nendza et al., 2016)] give the related literature. The top-10 attribution atoms is shown for ‘Atom-based’ method, and ‘Top-k’ denotes that the fragment ranks the k-th highest in the overall results for the molecule.

figures/si-fragment-16/si-fragment-16-eps-converted-to.pdf

Figure 17: **Figure S17. Attribution results of fragment-based method for ‘Endocrine disorders’ task (3/3).** The red highlight displays the crucial fragments or atoms for certain molecule. The three columns (from left to right) respectively denote the ‘Ground Truth’ fragment from the literature, the atom-based attribution result, and the fragment-based attribution result. References [19(Nendza et al., 2016)] give the related literature. The top-10 attribution atoms is shown for ‘Atom-based’ method, and ‘Top-k’ denotes that the fragment ranks the k-th highest in the overall results for the molecule.

figures/si-fragment-18/si-fragment-17-eps-converted-to.pdf

Figure 18: **Figure S18. Attribution results of fragment-based method for ‘Neoplasms benign, malignant and unspecified’ task (1/4).** The red highlight displays the crucial fragments or atoms for certain molecule. The three columns (from left to right) respectively denote the ‘Ground Truth’ fragment from the literature, the atom-based attribution result, and the fragment-based attribution result. References [9(Kazius et al., 2005), 20(Benigni & Bossa, 2008)] give the related literature. The top-10 attribution atoms is shown for ‘Atom-based’ method, and ‘Top-k’ denotes that the fragment ranks the k-th highest in the overall results for the molecule.

figures/si-fragment-181/si-fragment-181-eps-converted-to.pdf

Figure 19: **Figure S19. Attribution results of fragment-based method for ‘Neoplasms benign, malignant and unspecified’ task (2/4).** The red highlight displays the crucial fragments or atoms for certain molecule. The three columns (from left to right) respectively denote the ‘Ground Truth’ fragment from the literature, the atom-based attribution result, and the fragment-based attribution result. References [20(Benigni & Bossa, 2008), 21(Bailey et al., 2005), 22(Stepan et al., 2011)] give the related literature. The top-10 attribution atoms is shown for ‘Atom-based’ method, and ‘Top-k’ denotes that the fragment ranks the k-th highest in the overall results for the molecule.

figures/si-fragment-19/si-fragment-19-eps-converted-to.pdf

Figure 20: **Figure S20. Attribution results of fragment-based method for ‘Neoplasms benign, malignant and unspecified’ task (3/4).** The red highlight displays the crucial fragments or atoms for certain molecule. The three columns (from left to right) respectively denote the ‘Ground Truth’ fragment from the literature, the atom-based attribution result, and the fragment-based attribution result. References [20(Benigni & Bossa, 2008), 22(Stepan et al., 2011)] give the related literature. The top-10 attribution atoms is shown for ‘Atom-based’ method, and ‘Top-k’ denotes that the fragment ranks the k-th highest in the overall results for the molecule.

figures/si-fragment-20/si-fragment-20-eps-converted-to.pdf

Figure 21: **Figure S21. Attribution results of fragment-based method for ‘Neoplasms benign, malignant and unspecified’ task (4/4).** The red highlight displays the crucial fragments or atoms for certain molecule. The three columns (from left to right) respectively denote the ‘Ground Truth’ fragment from the literature, the atom-based attribution result, and the fragment-based attribution result. References [9(Kazius et al., 2005), 20(Benigni & Bossa, 2008)] give the related literature. The top-10 attribution atoms is shown for ‘Atom-based’ method, and ‘Top-k’ denotes that the fragment ranks the k-th highest in the overall results for the molecule.

figures/si-MGA/si-MGA-eps-converted-to.pdf

Figure 22: **Figure S22. Prediction performance comparison between multitask graph attention framework (MGA) and our fragment-based GCN method.** A) Prediction comparison of the six property tasks. For each property task, the left bar denotes the performance of the MGA framework, and the right one denotes the performance of the fragment-based method. The error line represents the variance of prediction performance. B) The detailed description of the six property tasks in A.

figures/si-MGA-1/si-MGA-1-eps-converted-to.pdf

Figure 23: **Figure S23. Crucial substructure mining results of MGA framework and fragment-based method for ‘Hepatobiliary disorders’ task.** The red highlights display the crucial fragments for certain molecule. The highlights of the left column and the right column represent ‘Ground Truth’ fragment from the literature, and the fragment-based attribution result. References [1([Smith et al., 2003](#)), 2([Usui et al., 2009](#)), 7([Wong et al., 2000](#))] give the related literature, and ‘Top-k’ denotes that the fragment ranks the k-th highest in the overall results for the molecule. The brown highlights in the middle column display the substructure obtained from multitask graph attention framework. The atoms with darker colors are more crucial.

figures/si-MGA-2/si-MGA-2-eps-converted-to.pdf

Figure 24: **Figure S24. Crucial substructure mining results of MGA framework and fragment-based method for ‘Congenital, familial and genetic disorders’ task.** The red highlights display the crucial fragments for certain molecule. The highlights of the left column and the right column represent ‘Ground Truth’ fragment from the literature, and the fragment-based attribution result. References [9(Kazius et al., 2005), 10(Bailey et al., 2005), 11(Benigni & Bossa, 2008), 13(Mariotti et al., 2013)] give the related literature, and ‘Top-k’ denotes that the fragment ranks the k-th highest in the overall results for the molecule. The brown highlights in the middle column display the substructure obtained from multitask graph attention framework. The atoms with darker colors are more crucial.

figures/si-MGA-3/si-MGA-3-eps-converted-to.pdf

Figure 25: **Figure S25. Crucial substructure mining results of MGA framework and fragment-based method for ‘Skin and subcutaneous tissue disorders’ task.** The red highlights display the crucial fragments for certain molecule. The highlights of the left column and the right column represent ‘Ground Truth’ fragment from the literature, and the fragment-based attribution result. References [14([Enoch et al., 2008](#))] give the related literature, and ‘Top-k’ denotes that the fragment ranks the k-th highest in the overall results for the molecule. The brown highlights in the middle column display the substructure obtained from multi- task graph attention framework. The atoms with darker colors are more crucial.

figures/si-MGA-4/si-MGA-4-eps-converted-to.pdf

Figure 26: **Figure S26. Crucial substructure mining results of MGA framework and fragment-based method for ‘Blood and lymphatic system disorders’ task.** The red highlights display the crucial fragments for certain molecule. The highlights of the left column and the right column represent ‘Ground Truth’ fragment from the literature, and the fragment-based attribution result. References [17([van N, 2003](#)), 18([Notley et al., 2002](#))] give the related literature, and ‘Top-k’ denotes that the fragment ranks the k-th highest in the overall results for the molecule. The brown highlights in the middle column display the substructure obtained from multi-task graph attention framework. The atoms with darker colors are more crucial.

figures/si-MGA-5/si-MGA-5-eps-converted-to.pdf

Figure 27: **Figure S27: Crucial substructure mining results of MGA framework and fragment-based method for ‘Endocrine disorders’ task.** The red highlights display the crucial fragments for certain molecule. The highlights of the left column and the right column represent ‘Ground Truth’ fragment from the literature, and the fragment-based attribution result. References [19(Nendza et al., 2016)] give the related literature, and ‘Top-k’ denotes that the fragment ranks the k-th highest in the overall results for the molecule. The brown highlights in the middle column display the substructure obtained from multitask graph attention framework. The atoms with darker colors are more crucial.

figures/si-MGA-6/si-MGA-6-eps-converted-to.pdf

Figure 28: **Figure S28. Crucial substructure mining results of MGA framework and fragment-based method for ‘Neoplasms benign, malignant and unspecified’ task.** The red highlights display the crucial fragments for certain molecule. The highlights of the left column and the right column represent ‘Ground Truth’ fragment from the literature, and the fragment-based attribution result. References [9(Kazius et al., 2005), 20(Benigni & Bossa, 2008)] give the related literature, and ‘Top-k’ denotes that the fragment ranks the k-th highest in the overall results for the molecule. The brown highlights in the middle column display the substructure obtained from multitask graph attention framework. The atoms with darker colors are more crucial.

References

- In vitro metabolism of tolcapone to reactive intermediates: relevance to tolcapone liver toxicity. (2003). *Chemical Research in Toxicology*, 16, 123–128.
- Evaluation of the potential for drug-induced liver injury based on in vitro covalent binding to human liver proteins. (2009). *Drug Metabolism and Disposition*, 37, 2383–2392.
- Conjugative metabolism of drugs. (2007). *Drug Metabolism in Drug Design and Development*, 3, 37–88.
- Studies on the metabolism of troglitazone to reactive intermediates in vitro and in vivo. Evidence for novel biotransformation pathways involving quinone methide formation and thiazolidinedione ring scission. (2001). *Chemical Research in Toxicology*, 14, 62–70.
- Oxidation of aminopyrine by hypochlorite to a reactive dication: possible implications for aminopyrine-induced agranulocytosis. (1995). *Chemical Research in Toxicology*, 8, 226–233.
- Inhibition of mitochondrial beta-oxidation of fatty acids by pirprofen. Role in microvesicular steatosis due to this nonsteroidal anti-inflammatory drug.. (1987). *Journal of Pharmacology and Experimental Therapeutics*, 242, 1133–1137.
- The role of mitochondrial injury in bromobenzene and furosemide induced hepatotoxicity. (2000). *Toxicology Letters*, 116, 171–181.
- Isoniazid and iproniazid: activation of metabolites to toxic intermediates in man and rat. (1976). *Science*, 193, 901–903.
- Derivation and validation of toxicophores for mutagenicity prediction. (2005). *Journal of Medicinal Chemistry*, 48, 312–320.
- The use of structure–activity relationship analysis in the food contact notification program. (2005). *Regulatory Toxicology and Pharmacology*, 42, 225–235.
- Structure alerts for carcinogenicity, and the Salmonella assay system: a novel insight through the chemical relational databases technology. (2008). *Mutation Research/Reviews in Mutation Research*, 659, 248–261.
- A critical assessment of the genotoxicity profile of the fungicide tricyclazole. (2020). *Environmental and Molecular Mutagenesis*, 61, 300–315.
- Furan: a critical heat induced dietary contaminant. (2013). *Food & Function*, 4, 1001–1015.
- Identification of mechanisms of toxic action for skin sensitisation using a SMARTS pattern based approach. (2008). *SAR and QSAR in Environmental Research*, 19, 555–578.
- Structure-activity relationships for skin sensitization potential: development of structural alerts for use in knowledge-based toxicity prediction systems. (1994). *Journal of Chemical Information and Computer Sciences*, 34, 154–161.
- Structural alert/reactive metabolite concept as applied in medicinal chemistry to mitigate the risk of idiosyncratic drug toxicity: a perspective based on the critical examination of trends in the top 200 drugs marketed in the United States. (2011). *Chemical Research in Toxicology*, 24, 1345–1410.
- In vitro hematotoxicity testing in drug development: a review of past, present and future applications. (2003). *Current Opinion in Drug Discovery & Development*, 6, 100–109.
- Bioactivation of tamoxifen by recombinant human cytochrome P450 enzymes. (2002). *Chemical Research in Toxicology*, 15, 614–622.
- Screening for potential endocrine disruptors in fish: evidence from structural alerts and in vitro and in vivo toxicological assays. (2016). *Environmental Sciences Europe*, 28, 1–19.

Structure alerts for carcinogenicity, and the Salmonella assay system: a novel insight through the chemical relational databases technology. (2008). *Mutation Research/Reviews in Mutation Research*, 659, 248–261.

The use of structure–activity relationship analysis in the food contact notification program. (2005). *Regulatory Toxicology and Pharmacology*, 42, 225–235.

Structural alert/reactive metabolite concept as applied in medicinal chemistry to mitigate the risk of idiosyncratic drug toxicity: a perspective based on the critical examination of trends in the top 200 drugs marketed in the United States. (2011). *Chemical Research in Toxicology*, 24, 1345–1410.